

Lawrence Berkeley National Laboratory

Lawrence Berkeley National Laboratory

Title

EUV extendibility: challenges facing EUV at 1x and beyond

Permalink

<https://escholarship.org/uc/item/3c845996>

Author

Naulleau, Patrick

Publication Date

2014-02-07

EUV extendibility: challenges facing EUV at 1x and beyond

Patrick P. Naulleau,¹ Christopher N. Anderson,¹ Suchit Bhattarai,² Andrew Neureuther²

¹Center for X-ray Optics, Lawrence Berkeley National Laboratory, Berkeley, CA, USA

²EECS, University of California, Berkeley, CA, USA

Extreme ultraviolet chemically amplified resist performance has recently been extended to the 15-nm half pitch regime, yet line-edge roughness (LER) remains far from targets. Stochastic analysis, however, shows current LER performance to be material limited rather than photon limited.

Interest in contact hole printing and contact size uniformity has dramatically increased over the past few years. As with line space printing, we find contact uniformity performance to be material limited rather than photon limited. Nevertheless, current resist parameters would lead to the photon noise alone exceeding the uniformity requirement by the 16-nm half pitch node with conventional masks. The use of phase shift masks is shown to provide a significant benefit. Combining phase shift masks with relatively modest improvements in resist is predicted to lead to target performance down to 12-nm half pitch and beyond.

Keyword: photoresist, extreme ultraviolet, shot noise, line-edge roughness

1. Introduction

Extreme ultraviolet (EUV) lithography has now entered the pilot line phase and interest in the question of extendibility to the 1x node and beyond has greatly increased. Advanced resist testing with 0.3 numerical aperture (NA) microfield exposure tools [1,2] is now focused on extremely low- k_1 configurations and development is underway for new 0.5-NA tools [3].

Chemically amplified resist performance has recently been extended to the 15-nm half pitch regime, yet line-edge roughness (LER) remains far from targets. Here we explore the importance of photon limits relative to materials limits for the current LER values. This analysis is also extended to contact critical dimension uniformity (CDU).

As we push to the deep 1x regime, resist performance cannot be considered in isolation of aerial image performance. Extending EUV to the low- k_1 regime will potentially come with significant implications on aerial image performance and thus variability. When

exploring variability limits, mask and system optimization should be considered.

2. Resolution status

Since achieving 16-nm half pitch (HP) performance in chemically amplified (CA) resists in 2011, progress in ultimate resolution has stalled. Figure 1 shows a plot of EUV resist resolution as a function of time. Despite the lack of progress in ultimate resolution, a sensitivity improvement from 30 mJ/cm² to 20 mJ/cm² was made between 2011 and 2012, however, at the cost of LER.

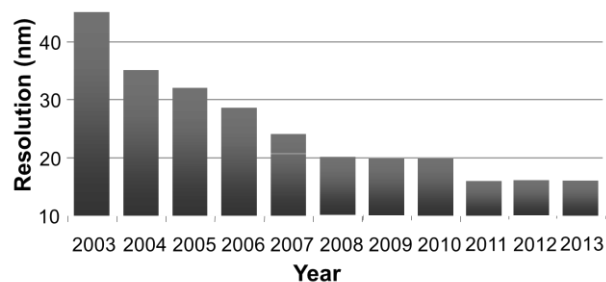


Figure 1. Progress in EUV chemically amplified resist resolution as a function of time.

Figure 2 shows the 16-nm HP patterning results for two difference CA resists using pseudo phase shift mask mode in the SEMATECH Berkeley Microfield Exposure Tool (MET) [4]. The sensitivity of resist A is 30 mJ/cm^2 and resist B is 20 mJ/cm^2 . The measured line-width roughness (LWR) is $3.1 \pm 0.1 \text{ nm}$ and $4.0 \pm 0.1 \text{ nm}$ for resists A and B, respectively [5]. Moreover we find the intrinsic LER to be $2.45 \pm 0.03 \text{ nm}$ and $3.28 \pm 0.03 \text{ nm}$ for resists A and B, respectively. Where we define the intrinsic LER as the LER on 50 nm lines and spaces. We also find the LER correlation length to be about 11 nm for both resists.

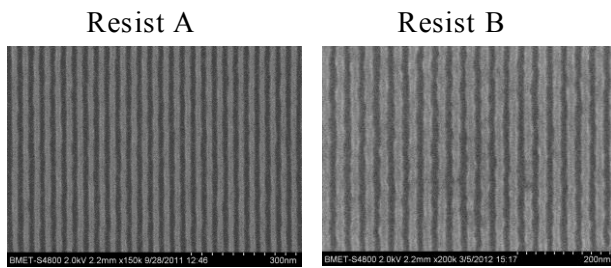


Figure 2. 16-nm HP patterning results for two difference CA resists using pseudo phase shift mask mode in the SEMATECH Berkeley MET.

Based on the known aerial image, resist absorptivity of approximately 0.004 nm^{-1} , the 30 nm film thickness and an assumed acid blur as determined from the measured LWR correlation length of 11 nm, one can use stochastic modeling [6-8] to predict the photon-noise limited LWR. For Resist A we predict a shot-noise limited LWR of $1.76 \pm 0.05 \text{ nm}$ and $2.12 \pm 0.04 \text{ nm}$ for Resist B. From these values we predict the material limited LWR to be 2.6 nm and 3.4 nm for Resists A and B, respectively. Even at 16-nm HP with conventional absorptivity and very thin resists, we find the experimental LWR results to be material limited instead of photon limited.

We note that the modeled photon limited LWR can be further improved through optimization of the resist blur. It can be shown that the optimal blur when considering equal lines and spaces is close to one half the half pitch [9]. Further applying this assumption to the stochastic model yields a predicted LWR of $1.52 \pm 0.03 \text{ nm}$ and $1.85 \pm 0.02 \text{ nm}$ for Resist A and B,

respectively. Even further reduction would be possible by increasing the assumed absorptivity beyond the conventional polymer value of 0.004 nm^{-1} .

Interest in EUV contact hole performance has dramatically increased over the last two years. As expected, contact resolution does not match line space resolution, but nevertheless significant progress has been made on this front as well. Figure 3 shows contact holes in two leading resists printed using quadrupole illumination on the SEMATECH Berkeley microfield exposure tool (MET).

Patterning down to 18-nm HP is demonstrated which represents the theoretical resolution limit for a 0.3-NA system operating with quadrupole illumination and a pole partial coherence of 0.12. Reducing the pitch beyond 36 nm would cause the diffracted orders to start clipping in the pupil. In Resist C we achieve a 3-sigma CDU of 3.9 nm at 39 mJ/cm^2 for 20-nm HP. For Resist A we achieve a 3-sigma CDU of 2.85 nm and 3.3 nm, for 20 and 18 nm HP contacts, respectively. The patterning dose is 70 mJ/cm^2 for both CDs.

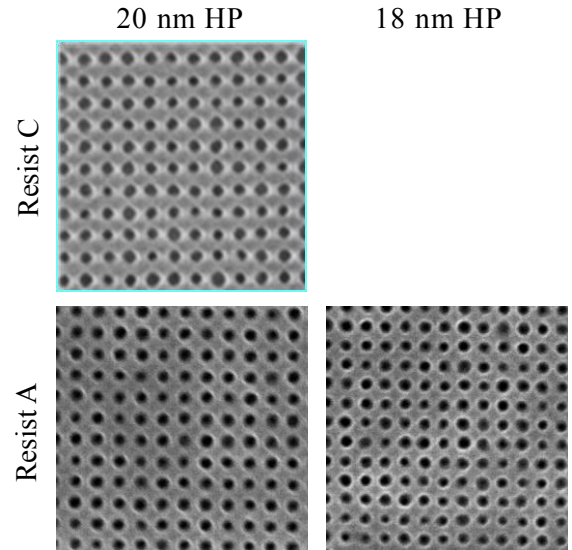


Figure 3. Contact holes in two leading resists printed using quadrupole illumination on the SEMATECH Berkeley (MET).

3. Contact CDU limiting terms

A significant concern with contact printing is CDU. Like LER, contact CDU is determined by many factors including photon shot noise. Here we apply a stochastic resist

model to the study of the relative importance of photon shot noise to current contact CDU performance.

For our experimental data, we rely on a comprehensive study performed by Neisser et al. published in these proceedings [10]. We expand on those results by applying a more comprehensive resist model than the “photon bucket” method used in Ref. [10]. The stochastic model we use starts with an aerial image calculation based on the known mask and optical parameters. As reported in [10] the HP is 26 nm and a mask bias of 20% is used. For dose we use the experimental values in [10], for absorptivity we use supplier provided data, and for acid blur we use values determined from best fit to the experimental exposure latitude. We fix the photo acid generator concentration at 0.3 nm^{-3} , the deprotection rate at $1 \text{ nm}^3/\text{sec}$ and the acid-base annihilation rate at $10 \text{ nm}^3/\text{sec}$. The resist thickness is 60 nm. Base concentration and quantum yield are left as free parameters and set based on fitting to the measured dose to size. The model CDU is determined through the analysis of 900 contacts yielding a theoretical error bar of 2.4% assuming Gaussian statistics.

Figure 4 shows a bar chart of the measured CDU compared to the predicted photon limited CDU and predicted total stochastic CDU which in addition to the photon stochastics includes acid noise, and photo acid generator and quencher distribution stochastics. As described in Ref. [10], what is reported as the measured CDU has been corrected for systematic mask and tool effects and thus is expected to represent only the resist contribution to the CDU. The results show the photon limit to be a relatively small contribution to the measured CDU, especially if we consider the fact that the various noise terms would be expected to add in quadrature.

To better visualize the relative importance of the various terms, Fig. 5 shows a stacked bar chart summing to the total measured CDU and breaking out the quadrature photon, material, and other effects, where other corresponds to phenomena not captured in the current stochastic model. Examples of such phenomena might include variations in number of protected sites, variations in development, and variations in diffusion. The

photon limit accounts on average for the only 9% of the observed CDU. On average, 86% of the CDU effect is unaccounted for in the model.

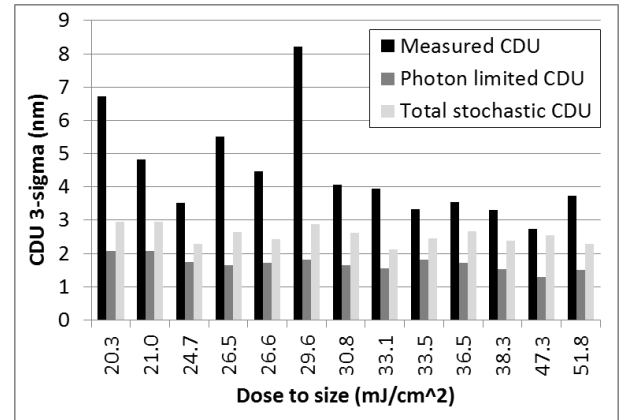


Figure 4. Bar chart of measured CDU compared to the predicted photon limited total stochastic CDU.

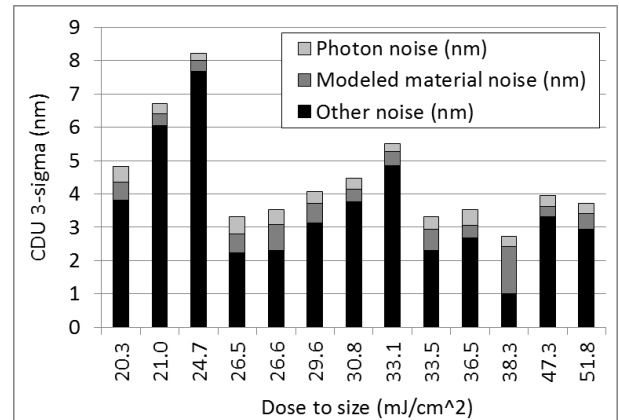


Figure 5. Stacked bar chart summing total measured CDU showing quadrature photon, material, and other effects. Other corresponds to phenomena not captured in the current stochastic model.

4. The contact CDU photon limit

Although the previous section showed photon noise to be an insignificant contributor to current contact CDU limits, explicitly considering the implications of the photon limit in the future is valuable. In this section we consider the impact of system, mask, and resist parameters on the photon limited contact CDU.

We start by considering the impact of resist blur on 16-nm contacts (Fig. 6). A 0.33 NA system with optimized quadrupole illumination is assumed. The remaining resist parameters are as defined in the previous

section, and we assume an absorptivity of 0.0042 nm^{-1} , a resist thickness of 50 nm, and a deprotection rate of $3 \text{ nm}^3/\text{sec}$. Unlike for lines and spaces, the results show continued improvement in CDU with decreasing blur. Thus, the optimal resist parameters for minimum contact CDU and minimum line-space LWR at the same CD do not match.

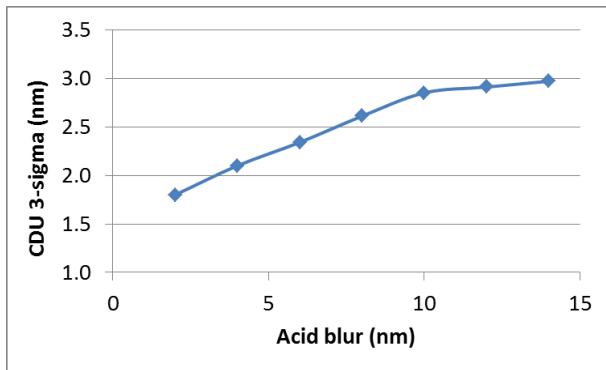


Figure 6. 16-nm dense contact CDU as a function of resist blur.

Next we consider the impact of mask bias on contact CDU (Fig. 7) under the same conditions as described above and assuming 4-nm acid blur. Since we are operating in 4-wave imaging mode and near the resolution limit, the primary effect of bias is simply to change the dose while keeping the CDU fixed. We see that a $2\times$ improvement in required dose relative to the zero bias case is possible with increasing positive bias (increase the size of the open contacts).

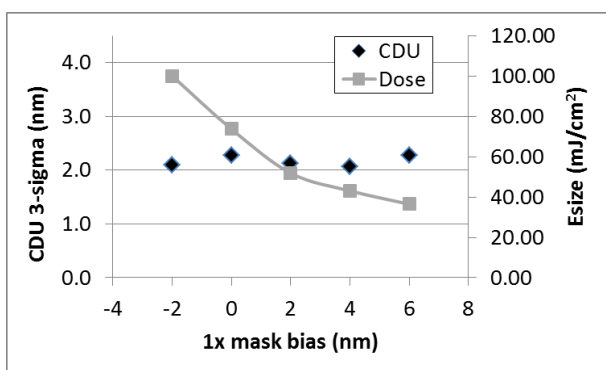


Figure 7. Contact CDU and required dose as a function of mask bias.

The results above show increased open area to be a big benefit. Taking this to its limit leads one to a brightfield mask which would require a negative tone resist. Figure 8 shows the computed CDU as a function of bias for

this configuration. Increasing bias corresponds to the dark contact increasing in size. In this case we see the dose increase and CDU decrease with increasing bias.

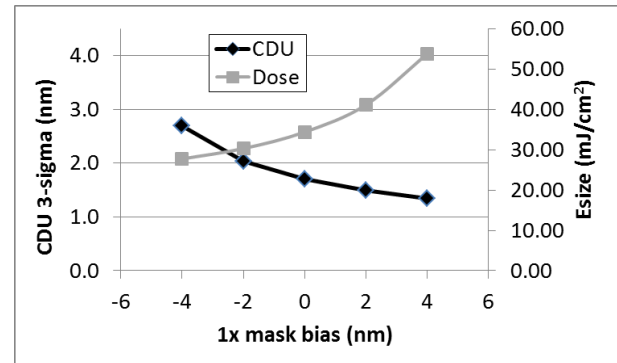


Figure 8. Contact CDU and required dose as a function of mask bias for the brightfield case.

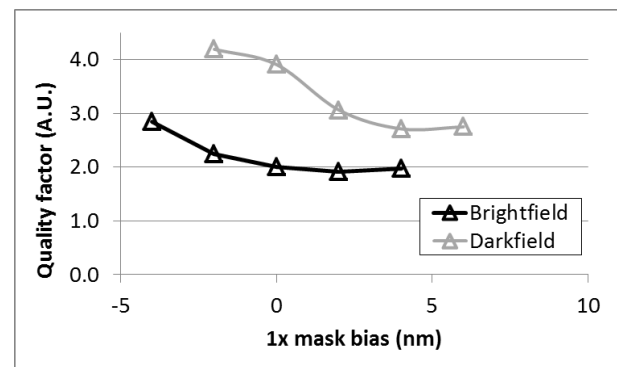


Figure 9. Contact printing quality factor for 16-nm contacts as a function of mask bias for both darkfield and brightfield processes.

As often done with LER analysis, it is useful to consider a relative quality metric such as the Z factor or Nano-Z factor metrics [11,12]. Here we define the quality factor as

$$CDU * \sqrt{\text{dose}} / [CD * 0.1 * 0.7 * \sqrt{20}] \quad [1]$$

where by definition we are setting the dose target to $20 \text{ mJ}/\text{cm}^2$. We have arbitrarily set the photon limited CDU target to 1.12 nm, leaving 30% for other terms to get a total CDU of 1.6 nm, or 10% of the CD. A value of 1 or smaller for the metric corresponds to the target performance or better. From this analysis (Fig. 9) we see that brightfield contacts with a negative tone resist process would be the ideal configuration for photon noise.

It is evident that increased bias improves the quality factor through improved optical

efficiency of the system. This indicates that we might be able to do even better using strong phase shift mask technology. Figure 10 shows the quality factor results for this configuration as a function of partial coherence. In this case we use on-axis illumination. Here we see both improved dose and improved CDU with decreasing sigma and can achieve a quality factor of 1.17.

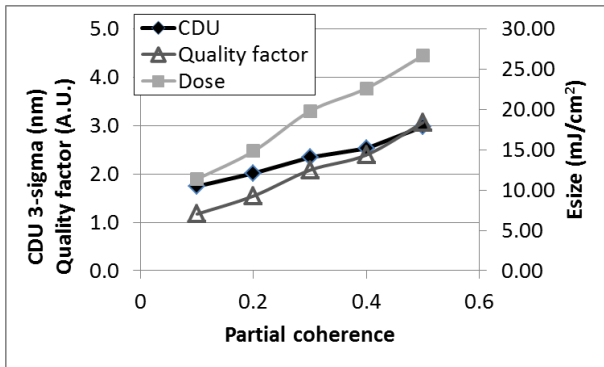


Figure 10. Contact printing quality factor for 16-nm contacts as a function of partial coherence assuming the use of a strong phase shift mask.

Next we consider the implications of photon limits for extensions beyond 16 nm. We note that this also requires a proportional increase in NA. We look at 14 nm and 12 nm requiring NAs of 0.38 and 0.44, respectively. We also assume the resist thickness to decrease proportionally. Figure 11 shows the quality factor for these two cases in addition to the 16-nm case for reference, considering the optimal brightfield and darkfield amplitude mask and phase shift mask conditions found above.

Figure 11 shows quality factors ranging from approximately 1 to 5 depending on the CD and mask type. From the definition of the quality factor, it is evident that achieving a quality factor of unity while keeping all other system and resist parameters fixed requires an increase in the number of absorbed photons that goes as the square of the quality factor. Certainly this cannot come from dose alone, but rather needs to come from increased photon absorption. Note that all the examples considered here assume conventional polymer resist absorptivity of 0.0042 nm^{-1} and a quantum yield (number of acids per absorbed photon) of 3. Clearly significant progress is required in photon efficiency in order to

achieve target performance for 12 nm contacts with conventional masks.

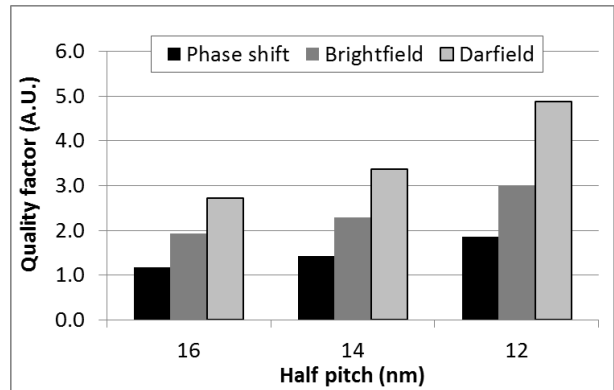


Figure 11. Contact printing quality factor as a function of half pitch for optimized phase shift, brightfield, and darkfield masks cases.

5. First order materials limit

Although a complete materials stochastic study is beyond the scope of this paper, it is useful to consider a few special cases; we start with acid noise. Because EUV photons are not selectively absorbed by photo acid generator, the acid statistics do not simply follow the absorbed photon statistics. Generation of the acids is itself a stochastic process that leads to a further degradation of the stochasticity even though the final acid count is larger than the absorbed photon count.

Figure 11 shows the relative importance of the acid noise compared to the photon noise as a function of quantum yield. We assume the optimal darkfield mask configuration and 14 nm HP contacts. We use the same resist parameters as used in the previous section, but scale the photo acid generator and quencher concentration proportionally to the quantum yield ensuring that saturation effects are kept constant as the quantum yield is varied. Under these conditions, the dose to size is seen to remain constant at 28 mJ/cm^2 and we can isolate the impact of the acid noise relative to the fixed photon noise by noting that the acid noise is a multiplicative factor on top of the photon noise and thus that the two standard deviations add in quadrature. The acid-limited CDU is also plotted in Fig. 12.

At a quantum yield of 3, we see the CDU to increase from 2.25 nm for photon noise only

to 2.58 nm when also including acid noise. The acid noise component alone is 1.26 nm. Note that the photo acid generator concentrations we have used corresponding to the plotted quantum yield values in Fig. 12 range from $0.1/\text{nm}^3$ to $0.6/\text{nm}^3$.

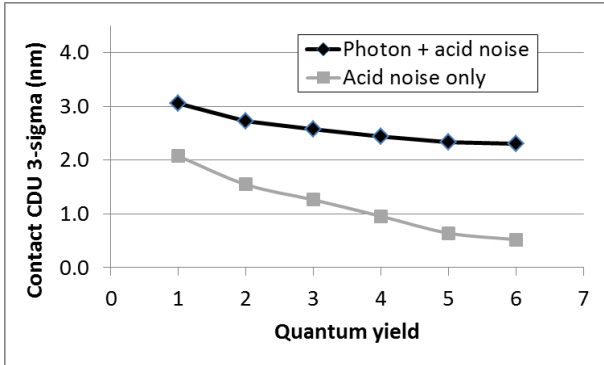


Figure 12. Contact CDU as a function of quantum yield considering the combine photon plus acid noise and the acid noise alone.

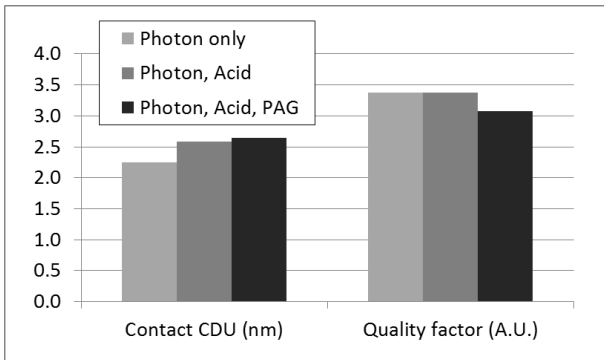


Figure 13. Comparison of CDU and quality factor for photon noise only and with the addition of acid and photo acid generator noise.

Finally, we briefly consider the relative importance of further materials stochastics, specifically photo acid generator stochastics. We again assume the optimal darkfield mask configuration and 14 nm HP contacts. The quantum yield is set to 3, photo acid generator concentration is 0.3 nm^{-3} , and the quencher concentration is 0.11 nm^{-3} . Figure 13 compares the CDU and the quality factor for the photon noise only, photon plus acid, and full materials stochastics cases. For the full materials case, we redefine the quality factor as

$$\text{CDU} \cdot \sqrt{\text{dose}} / [\text{CD} \cdot 0.1 \cdot 0.9 \cdot \sqrt{20}], \quad [2]$$

leaving 10% CDU for other unaccounted for terms. As expected, the CDU increases, however we see the quality factor to improve indicating simply that the material noise considered here accounts for less than 20% of the total CDU.

6. Prospects for the future

The CDU limitations presented above are based on typical resist parameters for today's resists. The question we ask in this section is: what might we achieve if these resist parameters could be pushed in the future? Perhaps the most obvious of these parameters is the resist absorptivity. For this we will assume that an absorptivity of 0.02 nm^{-1} can be achieved. We note that as reported by Stowers et al. [13], this has already been achieved with an inorganic EUV resist. For quantum yield, we will assume a value of 6 and note even higher values have been demonstrated by Brainard et al. [14]. For photo acid generator loading we will assume $0.5/\text{nm}^3$ noting that extremely high loading values have also been reported in [14]. For acid blur we will assume 3 nm and 2 nm for the electron blur.

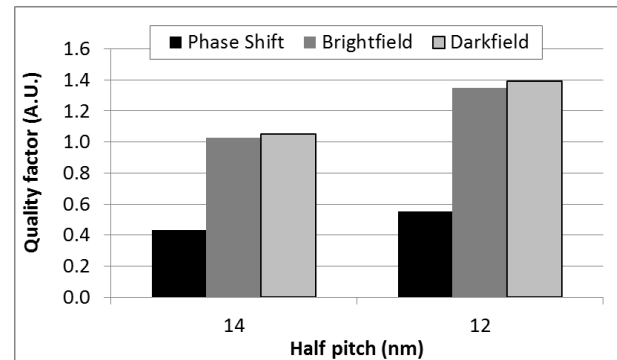


Figure 14. Quality factor for 14 and 12-nm HP with potential future improvements in absorptivity, quantum yield, and photo acid generator concentration.

Applying these conditions yields the results in Fig. 14 which shows the quality factor including photon, acid, and photo acid generator noise and the definition in Eq. [2] is used. For the phase shift mask we see a margin of nearly of factor of two even at 12-nm HP. For conventional masks, however, we see that 14-nm barely meets the

requirements, and that 12 nm would require an increase in dose of about 56% or further improved photon or acid efficiency.

7. Summary

As with line space printing, we have found contact uniformity performance to be material limited rather than photon noise limited. In the very best case, the unaccounted for material CDU is found to be 1 nm. Allowing the unaccounted for terms to occupy 10% of the total error budget, we see that it should be reduced to 0.6 nm for 14 nm contacts and 0.5 nm for 12 nm contacts.

Despite the present dominance of material effects, we also find that current resist parameters would lead to the photon noise alone exceeding the uniformity requirement by the 16-nm half pitch node with conventional masks. The use of phase shift masks, however, is shown to provide a significant benefit. In the absence of phase shift masks, we will need at least a 5× improvement in photon absorptivity and quantum efficiencies exceeding 6. Moreover, photo acid generator, or alternative, concentrations are predicted to need to exceed 0.5 nm^{-3} .

8. Acknowledgements

The authors are greatly indebted to the CXRO MET operations team including Gideon Jones, Lorie-mae Baclea-an, Mark Binenbaum, Chanin King, Gayan Pothuhera, Jessica Ritland, and Jessalyn Sincher. We also thank Ken Maruyama of JSR, Shinji Tarutani of Fuji, and Mike Wagner of Dow for excellent resist support, and Mark Neisser of SEMATECH for valuable discussions and experimental data support. This work was funded by SEMATECH and the authors thank Dominic Ashworth, Kevin Cummings, and Stefan Wurm for continued support of the SEMATECH MET exposure facility at the Advanced Light Source. The work was performed at Lawrence Berkeley National Laboratory's Advanced Light Source synchrotron facility and was supported by SEMATECH through the U.S. Department of Energy under Contract No. DE-AC02-05CH11231.

References

1. C. Anderson, D. Ashworth, L. Baclea-An, S. Bhattari, R. Chao, R. Claus, P. Denham, K. Goldberg, A. Grenville, G. Jones, R. Miyakawa, K. Murayama, H. Nakagawa, S. Rekawa, J. Stowers, P. Naulleau, "The SEMATECH Berkeley MET: demonstration of 15-nm half-pitch in chemically amplified EUV resist and sensitivity of EUV resists at 6.x-nm," Proc. SPIE **8322**, 832212 (2012).
2. Y. Tanaka, K. Matsunaga, S. Magoshi, S. Shirai, K. Tawarayama, and H. Tanaka, "Resolution capability of SFET with slit and dipole illumination," Proc. SPIE. **7969**, 79690Q (2011).
3. Glatzel, H. K., Ashworth, D., Bremer, M., Chin, R., Cummings, K., Girard, L., Goldstein, M., Gullikson, E. M., Hudyma, R., Kennon, J., Kestner, R., Marchetti, L. A., Naulleau, P. P., Soufli, R., Spiller, E. A., "Projection optics for EUVL micro-field exposure tools with a numerical aperture of 0.5", Proc. SPIE. **8679**, 867917 (April 2013) doi: 10.1117/12.2012698.
4. C. Anderson, D. Ashworth, L. Baclea-An, S. Bhattari, R. Chao, R. Claus, P. Denham, K. Goldberg, A. Grenville, G. Jones, R. Miyakawa, K. Murayama, H. Nakagawa, S. Rekawa, J. Stowers, P. Naulleau, "The SEMATECH Berkeley MET: demonstration of 15-nm half-pitch in chemically amplified EUV resist and sensitivity of EUV resists at 6.x-nm," Proc. SPIE **8322**, 832212 (2012).
5. 3σ LWR measured using SuMMIT LER analysis software covering a roughness period range from 16 nm to 407 nm with SEM noise bias removed.
6. G. Gallatin, "Resist blur and line edge roughness," Proc. SPIE **5754**, 38-52 (2005).
7. P. Naulleau and G. Gallatin, "The effect of resist on the transfer of line-edge roughness spatial metrics from mask to wafer," J. Vac. Sci. & Technol. B, **28**, 1259 (2010).
8. Stochastic modeling performed using SuMMIT LER analysis software (www.lithometrix.com)
9. D. Van Steenwinckel, J. Lammers, T. Koehler, R. Brainard, P. Trefonas, "Resist effects at small pitches," J. Vac. Sci. Technol. B **24**, 316 (2006); <http://dx.doi.org/10.1116/1.2151912>
10. M. Neisser, K. Cho, C. Sarma and K. Petrillo, "Understanding EUV Shot Noise: Comparing Theory and Requirements to Experimental Evidence," *these proceedings*.
11. T. Wallow, C. Higgins, R. Brainard, K. Petrillo,

- W. Montgomery, C. Koay, G. Denbeaux, O. Wood, Y. Wei, "Evaluation of EUV resist materials for use at the 32 nm half-pitch node," Proc. SPIE **6921**, 69211F (2008); doi:10.1117/12.772943
12. T. Younkin, et al., 2008 International Symposium on Extreme Ultraviolet Lithography, Lake Tahoe, CA, September 28-October 1, 2008, proceedings available from SEMATECH, Albany, NY.
 13. J. Stowers, A. Telecky, M. Kocsis, B. Clark, D. Keszler, A. Grenville, C. Anderson, P. Naulleau, "Directly patterned inorganic hardmask for EUV lithography," Proc. SPIE **7969**, 796915 (2011).
 14. R. Brainard, C. Higgins, E. Hassanein, R. Matyi, A. Wüest, "Film Quantum Yields of Ultrahigh PAG EUV Photoresists," J. Photopolym. Sci. Technol. **21**, 457-464 (2008).

DISCLAIMER

This document was prepared as an account of work sponsored by the United States Government. While this document is believed to contain correct information, neither the United States Government nor any agency thereof, nor The Regents of the University of California, nor any of their employees, makes any warranty, express or implied, or assumes any legal responsibility for the accuracy, completeness, or usefulness of any information, apparatus, product, or process disclosed, or represents that its use would not infringe privately owned rights. Reference herein to any specific commercial product, process, or service by its trade name, trademark, manufacturer, or otherwise, does not necessarily constitute or imply its endorsement, recommendation, or favoring by the United States Government or any agency thereof, or The Regents of the University of California. The views and opinions of authors expressed herein do not necessarily state or reflect those of the United States Government or any agency thereof or The Regents of the University of California.